UDC 681.5.014/.017

Ivan GOSPIĆ[1]
Ivanka BORAS[2]
Zoran MRAVAK[3]

Low-Temperature Ship Operations

Authors' Addresses (Adrese autora):

[1] *University of Zadar, Maritime Department,*
Mihovila Pavlinovića bb., 23000 Zadar, Croatia, e-mail: igospic@unizd.hr

[2] *University of Zagreb, Faculty of Mechanical Engineering and Naval Architecture*
Ivana Lučića 5, 10000 Zagreb, Croatia, e-mail: ivanka.boras@fsb.hr

[3] *Bureau Veritas, Direction Marine - Département Recherche*
Boulevard du Château - 92571 Neuilly sur Seine, Paris, France
www.bureauveritas.com, e-mail: zoran.mravak@bureauveritas.com

Received (Primljeno): 2011-05-23
Accepted (Prihvaćeno): 2011-06-27
Open for discussion (Otvoreno za raspravu): 2013-01-01

Original scientific paper

The article considers the design and operational problems inherent to vessels intended for operation in low-temperature environment. In doing so, emphasis is placed on the determination of ship's thermal responses for the purpose of proper selection of the construction materials of the hull and the equipment that are exposed to low temperature effects, and the heat capacity of the ship's thermal plant. In order to simulate in a reliable way the temperature response of relevant structures and unsteady heating loads of the typical ship spaces having a defined own microclimate in a realistic environment, the application of the concept of thermal networks in the modelling of thermal interactions is explained and is illustrated with examples. In this regard, an approach to the modelling of environmental items interacting with the ship, and to the modelling of thermal phenomena during the change of the aggregate state of the media involved by the acting thermal interactions is given.

Key words: *air frosting, ballast freezing, ice accretion, thermal networks winterization*

Rad broda u nisko-temperaturnom okruženju

Izvorni znanstveni rad

U članku se razmatra projektna i operativna problematika svojstvena plovilima namijenjenim službovanju u nisko-temperaturnom okruženju. Pri tom se naglasak stavlja na određivanje termalnih odziva broda sa svrhom pravilnog izbora konstrukcijskih materijala trupa i opreme izloženih nisko-temperaturnim utjecajima, kao i kapaciteta brodskoga toplinskog postrojenja.

Radi vjerodostojnoga simuliranja temperaturnih odziva strukture, te neustaljenih toplinskih opterećenja karakterističnih, mikroklimatski, definiranih brodskih prostora u realističnom okruženju, objašnjava se i primjerima ilustrira primjena koncepta toplinskih mreža u modeliranju nastupajućih toplinskih interakcija. S tim u vezi, dan je pristup modeliranju karakterističnih okolišnih veličina koje su u interakciji s brodom, kao i pristup modeliranju toplinskih fenomena tijekom promjene agregatnoga stanja toplinskim interakcijama obuhvaćenih medija.

Ključne riječi: *nanosi leda, stvaranje inja, termalne mreže, vinterizacija, zaleđivanje balasta*

1 Introduction

The motivation for writing this review came from a pronounced interest of the shipping and shipbuilding industry for ships assigned to work in a low-temperature environment. In principle there are two dominant low temperature problems; those related to the ships carrying very low-temperature liquefied cargo (ethylene, LNG-liquefied natural gas), and those related to all vessels intended for the service in a low temperature environment such as the Arctic [1].

The review is focused on the influence of the low-temperature surroundings on the ship's structure and on the occurrence of the ballast freezing. The safe operation of the vessel in the low temperature environments implies an adequate selection of the material for the ship's hull and the equipment, as well as a sufficient heating capacity of the thermal plant in order to balance the overall acting heating loads in the extremely harsh environmental conditions.

This paper presents a methodology for assessing the loads caused by low temperatures. The proposed method involves the consideration of the physical and operational aspects, with emphasis on the dominating influence of the thermal interactions occurring between the hull and the low temperature environment, which includes wet air, sea, sea ice and snow.

In addition, important aspects which must be taken into consideration are thermal interactions among different temperature items that are contained inside the ship, so this review presents a general approach to the mathematical modelling of the overall thermal interactions that occur during shipping.

The paper presents an approach to solving a very complex thermal problem by defining a system of many nonlinear differential equations, and further shows that such a complex system can be solved in real time using appropriate mathematical tools such as the software program *Mathematica 7*. Its application is illustrated by the example of an almost realistic modelling of thermal interactions between the oil tankers with double hull and low temperature environments during navigation through the Arctic.

2 Specifics of shipping through the Arctic region

2.1 Economic and maritime character of the Arctic region

In the past few years enormous reserves of oil and gas have been discovered on land and at sea, particularly in the Barents and Kara Seas. Therefore, much attention has been focused on this part of the Arctic region (AR). It has been estimated that up to 25 % of the world's undiscovered gas reserves lie in this area [2], [3].

It is envisaged that these discovered gas fields will be developed by using a combination of gas networks (mainly for the European gas market) and maritime transport with a considerable number of LNG carriers (mainly for the North-Western European and North American gas market) Figure 1a [2]. These ships will operate in severe weather conditions characterized by very low air temperatures, and in some parts of the route will be navigating through ice-covered sea either during the winter months or all year round.

In addition, the Northeast Passage or the Northern Sea Route (length around 6920 *nm*), as shown in Figure 1b., has been for 100 years reflected as an achievable shipping shortcut between Europe and the Far East (the route through the Suez Canal is about 11 430 *nm*). In this context since the end of the 19th century, Russia has put considerable efforts in developing the infrastructure of maritime transport through its respective part of the AR, resulting in the acquisition of significant experience in the organization of Arctic navigation [4] – [6].

Extreme climatic conditions in the AR impose substantial requirements for the ship and the crew and represent a significant challenge in performing maritime operations, mainly due to very low air temperatures (LAT), strong winds, freezing precipitation, frozen and slippery work surfaces and reduced visibility due to shortened daylight or complete absence of daylight as well as usually foggy winter days [7].

Average min. daily air temperatures (DAT) along the coasts of the Russian and Canadian Arctic during winter months vary between -50 ^{0}C and -45 ^{0}C, as is illustrated by the blue line in Figure 2a. [9]. Due to close monthly fluctuation of the mean DAT between average max. and min. DAT values, as shown in Figure 2b., as well as DAT fluctuations, the LAT close to -65 ^{0}C can occur [9], [10].

During the summer, one or two storms having velocities above 15 m/s often occur, but during the winter, the windstorms that are

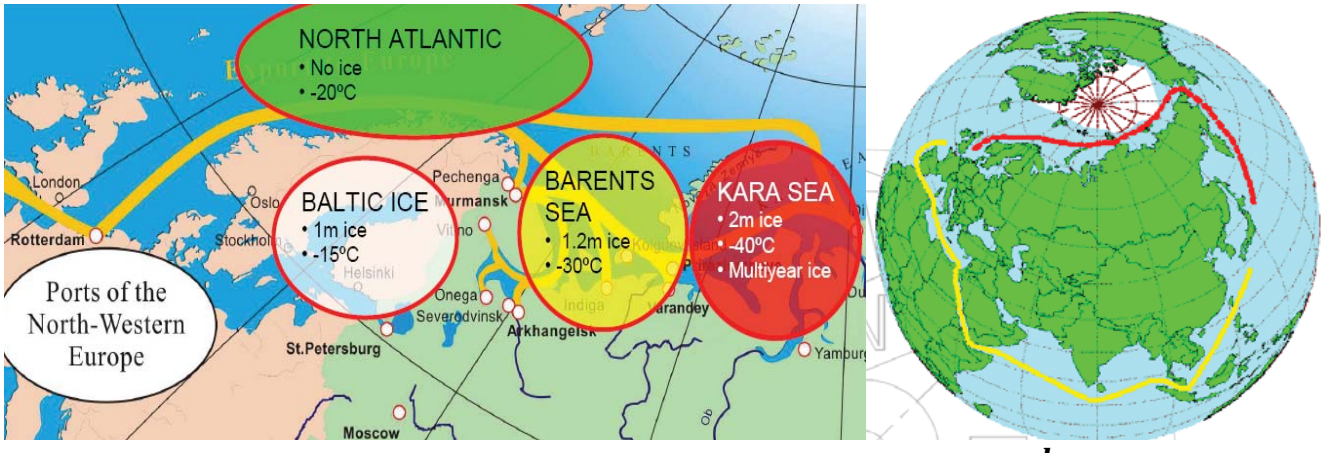

a *b*

Figure 1 a. **Shipping route from the Barents and Kara Seas,** b. **The Northern Sea Route**
Slika 1 a. **Trgovačka ruta iz Barentsova i Karskog mora,** b. **Sjeverna ruta**

Figure 2 a. **Average, max. and min. DAT at Litke (Kara Sea) [8],** b. **Mean DAT at Resolute (Canadian Arctic) [9]**
Slika 2 a. **Prosječne, maks. i min. DAT za Litke (Karsko more) [8],** b. **Srednje DAT za Resolute (kanadski Arktik) [9]**

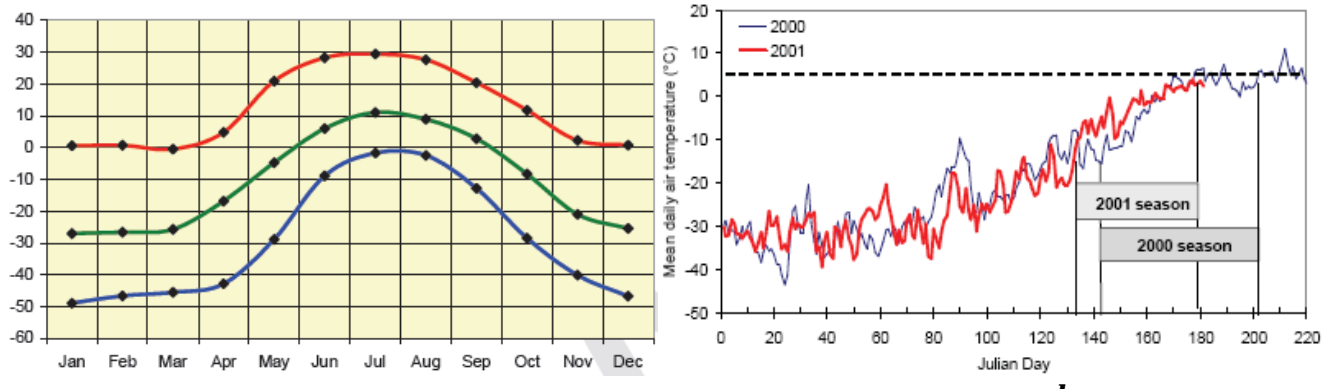

a *b*

very intense, reaching 30 m/s or occasionally even more, with a usual duration of only 6 to 12 hours (in some areas to four days) occur. In addition, the waves higher than 5 m are rare during the summer, but in the winter, the wave height can exceed 7-9 m. Further, although the first-year ice is dominant in the AR with a mean ice thickness up to 1.5 m, the southern Barents Sea may be ice-free until the middle of February, when thickness of the ice cover reaches more than 1.2 m maintaining the ice growth until May, whilst summer ice melting in the North Kara Sea is very slow, and very often the ice cover remains for the second year or longer, so that it makes the navigation along these areas hazardous and sometimes impossible [11].

Due to the decrease of the ice cover in the AR, the spray icing of ships and platforms i.e. *ice accretions* (IA) may be more frequent and more severe in the coming years than it has been in the past. Thus, the ice accumulates as an ice-water-air mixture with a density depending on the weather conditions on the vessel location ($\rho_{ia} \approx 850\,\mathrm{kg/m^3}$), as shown in Figure 3 [15]. Snow presents an additional problem. If it is accumulated and frozen, it can build to 100 mm of solid ice or 300 mm and more of porous ice, and consequently can cause local overstressing or reduction of overall stability by increasing topside weight and the areas exposed to wind [16].

Figure 3 **Ice accretions on the deck of a tanker**
Slika 3 **Nanosi leda na palubi tankera**

2.2 Main problems involved in shipping through the AR

It is apparent that tankers and LNG carriers operating in the extreme cold weather conditions of the AR are exposed to unique risks, and owing to the Classification Societies, new winterization guidelines are being established to meet the challenge of maintaining the necessary level of safety and environmental protection for the operation of these ships [12]-[14].

As very LAT are expected to be encountered by the ship during the voyage or in port, from the engineering point of view there are several of design and operational items that need to be considered. In terms of low temperature influences, the Design Service Temperature (DST) representing average min. DAT will be used.

When the ship is sailing in ballast condition through the harsh environment, ballast freezing (BF) in unheated double side ballast tanks (DSBT) above the ballast waterline will occur. In such conditions, even in cases where the tank itself does not freeze completely, thick ice formation or complete blockage within vent pipes due to air frosting (AF) has also been noted. Although extracted ice in the tank where freezing has occurred acts as an insulating layer reducing the heat load, freezing must be prevented because ice represents a weight that may not be discharged when the vessel is loaded, reducing the deadweight capacity. Thus, when DST is less than -30 ^{0}C, the steam heating coils are required to be installed for ballast heating in the fore and after peak, as well as in the DSBT.

In addition, there are also other problems that must be considered. They include the following: selection of steel grades for the structural parts exposed to very low temperatures (especially for LNG carriers), maintaining of liquid cargoes at the assigned storage temperatures (crude oil, heavy and marine diesel oil, lubrication oil, etc), providing heating and ventilation in the accommodation spaces such that at the DST the air temperature in the accommodation spaces is not less than 20 ^{0}C, pre-heating of the combustion air for prime movers to permit proper functioning of the their equipment, etc.

2.3 The acting thermal interactions between the ship and the environment

In terms of assessing the modelling of thermal interactions between the ship and the environment, it is necessary to assign distinguished physical models (PM) of ship's compartments to characteristics modes of the thermal interactions that are appearing in the realistic surroundings.

Regarding the overall thermal interactions between the ballast and its surroundings, it is necessary to consider several essentially different PM. During the navigation in ballast condition through different climatic regions characterized by intermittent environmental parameters changing in a wide range of values (air and sea temperatures, wind, insolation, etc.), the heat load of the ship's compartment is continuously changed, and consequently various physical processes such as internal AF, outside IA, and eventually BF if ballast heating coils have not enough capacity, occur.

Models without AF, IA, BF and radiation effects

The simplest PM that is shown in Figure 4, presents the symmetric thermal system of a double skin tanker in the ballast (DSTiB) that contains the cargo tank filled up with air or inert gas of unsteady temperature $T_3(t)$, P&S double bottom and DSBT containing ballast and air of unsteady temperatures $T_1(t)$, $T_2(t)$, $T_5(t)$ and $T_4(t)$, respectively. The symmetric thermal system is only valid when overall environmental vector quantities acting on the ship are complement with its longitudinal symmetric plane and when P&S ballast tanks are equally filled. In this case, it is assessed that inside AF and BF, as well as outside IA, do not occur and further the only convective and conductive mechanisms of heat transfer are taken into account, whilst long and shortwave radiation heat transfer is neglected.

So, taking into account unsteady temperatures of the atmospheric air $T_a(t) = T_7(t)$ and sea $T_S(t) = T_6(t)$, between the ballast in the DSBT indexed by $\boldsymbol{i}$, and some surrounding item indexed by $\boldsymbol{j}$, the unsteady heat load $\Phi_{1j}(t)$ will appear. Besides that, due to the existence of the mechanical and thermal imbalance between the air in the tank and the environment, the convective streaming

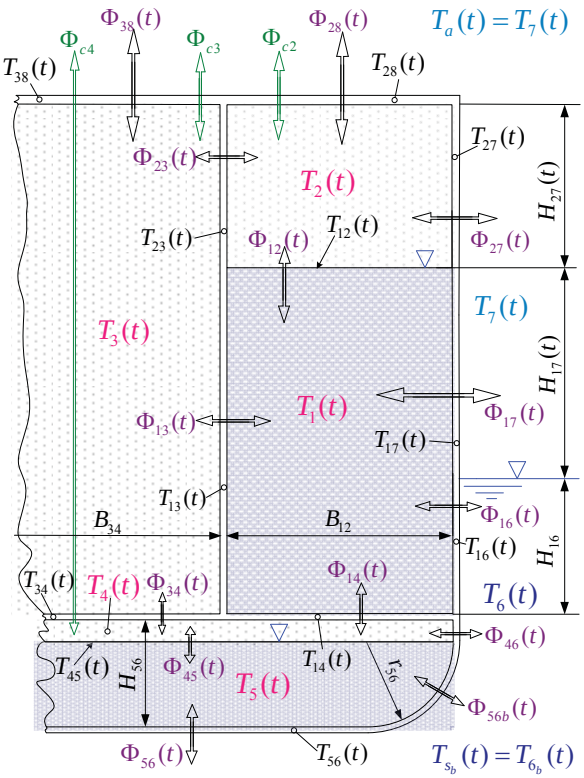

Figure 4 **The simplest PM of DSTiB**
Slika 4 **Najjednostavniji PM za DSTiB**

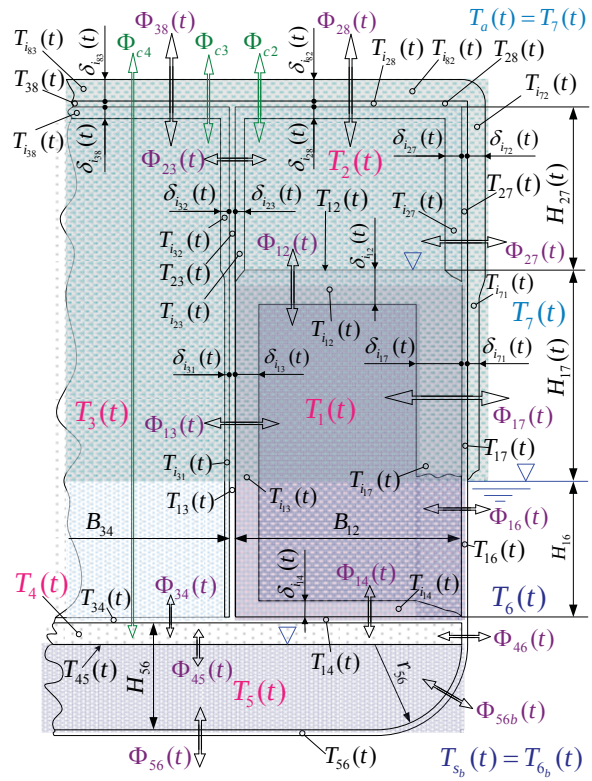

Figure 5 **The PM of the DSTiB with AF, IA and BF**
Slika 5 **PM za DSTiB s AF, AI i BF**

Figure 6 **The PM of the DSTiB with radiation effects**
Slika 6 **PM za DSTiB s radijacijskim utjecajima**

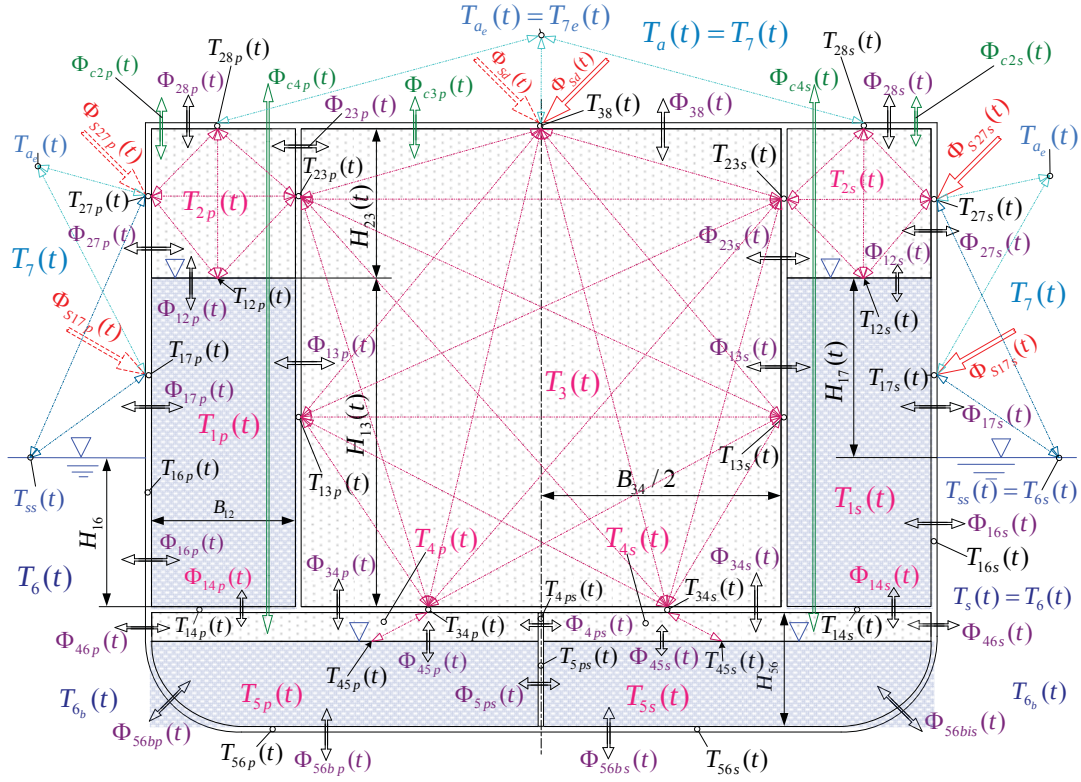

of the air through the corresponding vent system that induces adequate heat flow $\Phi_{c_j}(t)$ will occur.

Models taking into account AF, IA and BF

When navigating in ballast condition, a large part of the DSBT is in contact with the environmental air, having thus the lowest temperature among all surrounding items, and in this case the lowest temperature of the ballast occurs at the internal side wall surface. In the case of LNG carriers, the lowest temperature of the ballast may appear at any contact surface that divides the ballast tank from the cargo containment space. Figure 5 presents the ballast tanks arrangement in some tanker when the freezing process of the inadequately heated DSBT is in progress. The BF starts on the contact plating having the lowest temperature i.e. at the shell plating of the freeboard designated with number ***17*** that is in contact with the atmospheric air.

This model may be interesting for precise dynamic simulations of the BF in the extreme harsh environment and, based on it, the max. thickness of the ice extracted from the ballast can be estimated, and its influence on increasing stresses in the structural elements can be determined too. Besides that, when extreme environmental items are returned to their average values, better insight in the possibility of ballast defrosting by the existing heating system is achieved. However, even if BF is prevented in the harshest conditions, both AF in the top DSBT and IA due to the influence of the sea waves, wind and extracting frost from the atmospheric air on the outside under-cooled surfaces, may occur.

Models taking into account radiation effects, without AF, IA and BF

In case of an asymmetric heating load inside the considered ship section, as shown in Figure 6, which is a consequence of the acting solar insolation and of unequally filled P&S ballast tanks, the thermal imbalance between P&S ballast tanks must be taken into account. Besides, by convection and conduction, reasonable heat amounts are transported by the longwave radiation occurring between the different tempered walls through the spaces containing transparent media like air. There are also heating gains of the components of solar radiation on exposed surfaces. Due to that, all quantities on the portside are marked with indices ***p***, whilst those on the starboard are marked with indices ***s***.

This model is interesting when it is advisable to model the thermal interactions between some ship's compartment and relating surroundings, in order to estimate the acting of the accumulated heat in the compartment on the delay of the relating extreme responses, such as minimum ballast temperature in the harshest environmental conditions.

3 Modelling of overall thermal interactions between the ship and the surroundings

3.1 Dynamic thermal network concept (DTN) for thermal interactions modelling

The application of dynamic thermal networks (DTN) for the modelling of thermal interactions between the ship compartments having different temperatures and the surroundings is presented in this section. In general, the application of DTN allows the systematic formulation and solution of general and complicated thermal problems appearing throughout the ship by establishing and solving a corresponding system of differential equations. Further, it is also explained how to apply a DTN concept that includes the overall thermal interactions between different-temperature spaces and how to establish the corresponding equations [17], [18].

In this approach, a conditioned ship compartment surrounded with ***n*** different compartments that are composing a finite number of parts ***n***, called *nodes*, each of which is assumed to be isothermal and has its own heat capacity (capacitance). For a realistic modelling of thermal interactions, the capacitance is assigned to each node, and thus created nodes are further interconnected

Figure 7 **The PM of flat wall and the corresponding DTN branch**
Slika 7 **PM ravne stijenke i odgovarajuća grana DTN**

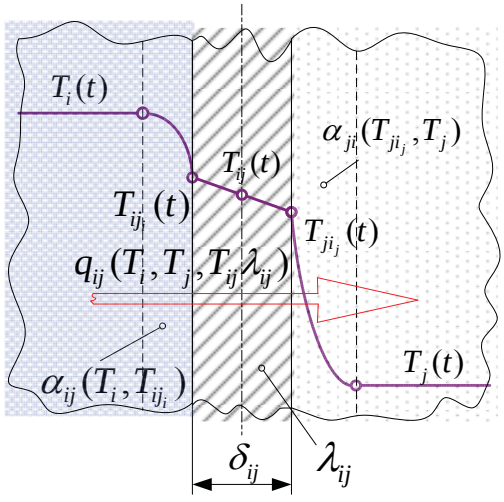

a. Physical model of the one – layer wall

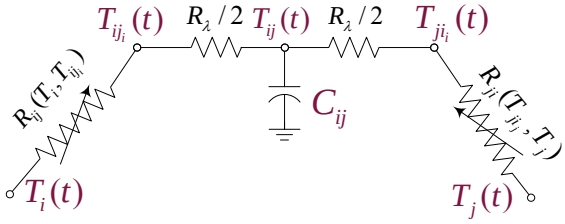

b. Dynamic thermal network branch

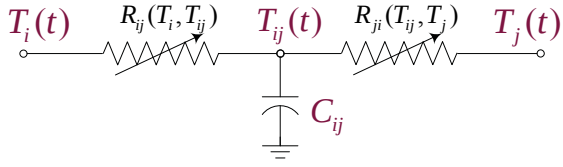

c. Simplified dynamic thermal network branch

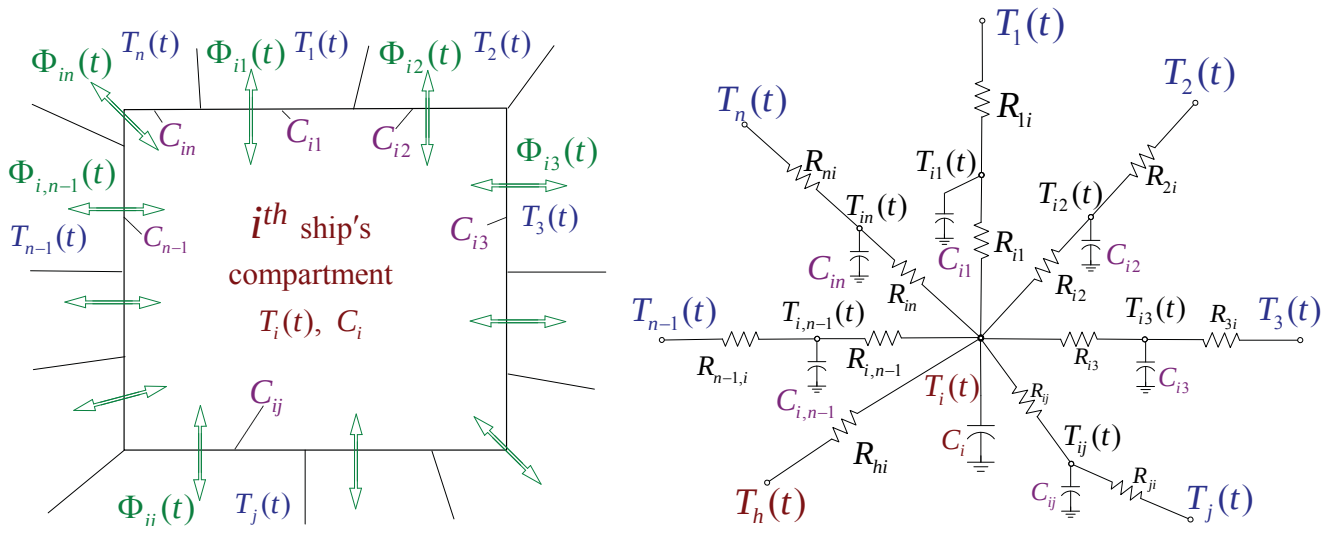

Figure 8 **Simplified DTN of a conditioned ship's compartment**
Slika 8 **Pojednostavnjena DTN klimatiziranog brodskog prostora**

with corresponding resistances (conduction, convection and/or radiation), making an appropriate DTN, as it is shown in Figure 7 for a flat fluid-tight wall.

As the walls of the ship compartments are thin and have relatively high thermal conductivity, the conductive thermal resistances (CTR) are negligible and the temperatures through them are close to constant $T_{ij_i}(t) \approx T_{ji_i}(t) = T_{ij}(t)$, and therefore the inner and outer convective thermal resistance (COTR) can be expressed in dependence on the temperatures $T_i(t)$ and $T_{ij}(t)$, i.e. $T_j(t)$ and $T_{ij}(t)$. Such a simplified dynamic thermal network branch (DTNB) is shown in Figure 7c.

By using DTNB for each ij^{th} one-layer wall having the capacitance C_{ij} and unsteady temperature $T_{ij}(t)$, the thermal interactions between the i^{th} ship's compartment filled up with a nontransparent fluid having the capacitance C_i and temperature $T_i(t)$ and n_i different compartments filled up with corresponding nontransparent fluids having unsteady temperatures $T_{ij}(t)$ and negligible capacitances can be drawn as illustrated in Figure 8.

Other characteristic items in Figure 8 are as follows: R_{ij}, R_{ij} are thermal resistances between the i^{th} media and the ij^{th} wall, i.e. between the ij^{th} wall and the j^{th} media, $\Phi_{ij}(t)$ is unsteady heat flow between the i^{th} and j^{th} media, $T_{h_i}(t)$ is temperature of the heating media intended for balancing of the overall heating load of the i^{th} compartment, whilst R_{hi} is thermal resistance between the heating media and the i^{th} media.

From this simplified DTN, by using general Kirchhoff's law for the flow in each node having capacitance, a system of nonlinear first order differential equations involving $n_i + 1$ unknown temperature functions is established, as follows:

$$\left.\begin{aligned} C_i \frac{dT_i(t)}{dt} + \frac{T_i(t) - T_{h_i}(t)}{R_{h_i i}(T_i, T_{h_i})} + \sum_{j=1}^{n_i} \frac{T_i(t) - T_{ij}(t)}{R_{ij}(T_i, T_{ij})} = 0 \\ C_{ij} \frac{dT_{ij}(t)}{dt} + \frac{T_{ij}(t) - T_i(t)}{R_{ij}(T_i, T_{ij})} + \frac{T_{ij}(t) - T_j(t)}{R_{ji}(T_{ij}, T_j)} = 0,\ \ j = 1,2,...,n_i \end{aligned}\right\} \quad (1)$$

As the COTR generally depends on the unknown temperature of media and contact wall surface, the corresponding system of differential equations is nonlinear and solvable exclusively by an adequate numerical method. For instance, using the empirical expressions for the convective heat transfer coefficient (CHTC) for a horizontal flat plate [19], and using numerical *sign* function by which the heat flux facing is taken into account, the following expression for CHTC is obtained:

$$\alpha_{ij}(T_i, T_{ij}) = 0{,}27 \frac{\lambda_i(T_i, T_{ij})}{L_{cij}} \left[\frac{g(T_{ij} - T_i)[1 - \text{sign}(T_i - T_j)]}{\upsilon_i(T_i, T_{ij}) a_i(T_i, T_{ij})(T_i + T_{ij})} \right]^{\frac{1}{4}} + \\ + 0{,}15 \frac{\lambda_i(T_i, T_{ij})}{L_{c_{ij}}} \left[\frac{g(T_i - T_{ij})[1 + \text{sign}(T_i - T_j)]}{\upsilon_i(T_i, T_{ij}) a_i(T_i, T_{ij})(T_i + T_{ij})} \right]^{\frac{1}{3}} \quad (2)$$

In this expression g is gravitational acceleration, and $L_{c_{ij}}$ is characteristic length that is defined by the formula $L_{c_{ij}} = A_{ij} / (2P_{ij})$, where A_{ij} is flat plate area and P_{ij} is its perimeter. The physical properties of the i^{th} media are $\lambda_i(T_i, T_{ij})$ thermal conductivity, $a_i(T_i, T_{ij})$ thermal diffusivity and $\upsilon_i(T_i, T_{ij})$ kinematics viscosity, and each of them is determined for the mean temperature $\bar{T}_{i,ij} = (T_i + T_{ij})/2$. By using table values for the physical properties of the media, the approximate expressions enabling analytic formulation of the thermal interactions in any conditions can be created. For instance, based on the above mentioned, the dependence of the CHTC on the temperatures of the media and contact surface is achieved, as shown in Figure 9 [1].

The temperature-dependent total thermal resistances $R_{ij}(T_i, T_{ij})$ and $R_{ji}(T_{ij}, T_j)$ (convective + conduction), for the case of natural convection are defined as follows:

$$R_{ij}(T_i, T_{ij}) = \frac{1}{A_{ij}(t)\alpha_{ij}(T_i, T_{ij})} + \frac{\delta_{ij}}{2\lambda_{ij} A_{ij}(t)} \quad (3)$$

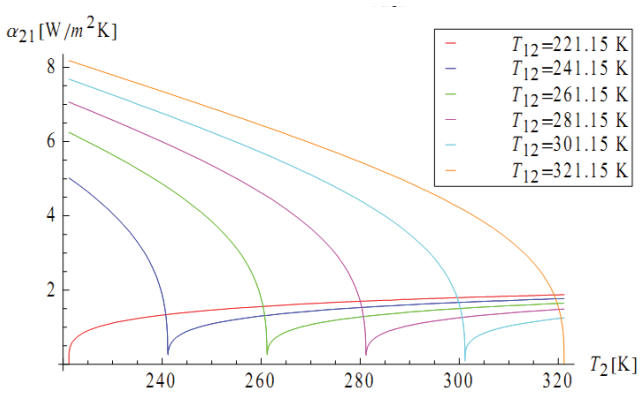

Figure 9 **The CHTC for a horizontal flat plate**
Slika 9 **CHTC za horizontalnu ravnu ploču**

$$R_{ji}(T_{ij},T_j)=\frac{\delta_{ij}}{2\lambda_{ij}A_{ij}(t)}+\frac{1}{A_{ij}(t)\alpha_{ji}(T_{ij},T_j)} \tag{4}$$

Thermal capacitances C_i and C_{ij} are defined by the following formula respectively,

$$C_{ij}=c_{ij}m_{ij}=f_{ij}\rho_{ij}A_{ij}\delta_{ij} \tag{5}$$

$$C_i(t)=c_i\rho_i V_i(t) \tag{6}$$

where C_{ij} is specific heat capacity and m_{ij} is mass of the wall, δ_{ij} and A_{ij} are steel plate thickness and area respectively, ρ_{ij} is steel density, and $f_{ij}\approx 1{,}1\div 1{,}15$ is a factor by which the mass of the stiffeners is taken into account, and c_i, ρ_i and $V_i(t)$ are specific heat capacity, density, and volume of the i^{th} media, respectively.

The unsteady heat flow indexed by ij_i appearing between media in the i^{th} compartment and fluid-tight wall is defined by the expression

$$\Phi_{ij_i}(t)=\frac{T_i(t)-T_{ij}(t)}{R_{ij}(T_i,T_{ij})} \tag{7}$$

while the total heating load of the i^{th} media is defined by the expression

$$\Phi_{tot_i}(t)=\frac{T_{h_i}(t)-T_i(t)}{R_{h_ii}(T_i,T_{h_i})}=C_i\frac{dT_i(t)}{dt}+\sum_{j=1}^{n_i}\frac{T_i(t)-T_{ij}(t)}{R_{ij}(T_i,T_{ij})} \tag{8}$$

3.2 Extension of the DTN concept to the modelling of thermal interactions onboard ships

The application of the above mentioned concept of DTN for modelling the thermal interactions between a tank and its surroundings is valid only in the case when the tank is filled up with nontransparent fluid having a fixed mass and unchanging aggregate state.

If a ship's compartment is a tank intended for the storage of liquid, then for safety reasons it must not be fully filled up with the liquid, but in its upper part a vapour mixture is contained. By means of the conducting system the vapour mixture is connected to the corresponding system for its treatment or is released to atmosphere. For instance, loaded LNG tanks contain the amount of LNG that corresponds to about 98 % of the tank volume, while the remaining tank volume contains the vapour mixture consisting predominantly of the LNG vapour and a minor part of the nitrogen vapour that remained in the tank after inerting sequences [20]. On the other hand, ballast tanks that must not be filled up with ballast, in their upper parts contain wet air that is connected by the vent system with the atmosphere.

Generally, regarding the thermal interactions modelling, each partly filled tank should be divided into two different artificial compartments, whereat it is preferable to accept the contact surface between the contained media (liquid and gas or vapour mixture) as an artificial one-layer wall. Such an artificial wall has no thermal capacitance, neither heat conductance exists, but only convective heat transfer between the existing media occurs, and there is also radiation heat transfer between the liquid media and the nontransparent surroundings.

In view of the overall thermal interactions modelling, it is evident that in the ship compartments, especially in the cargo and ballast tanks, the geometry of the surfaces contacting with the fluid is changed. These geometric sizes can be understood as variable thermal interfaces that participate in the accumulation and transfer of the heat, as well as in the processes involving the changes of the aggregate state of media.

For considering the real situation in a tank containing a variable mass of fluid due to its inflow and outflow, the usage of macroscopic laws of mass and energy for the nonisothermal systems will be necessary. Thus for the i^{th} compartment having p_i inlets and p_o outlets, the unsteady-state macroscopic balances of the mass and energy take the form as follows [20]:

$$\frac{dm_i(t)}{dt}=\sum_{i=0}^{p_i}\dot{m}_{i_i}(t)-\sum_{o=0}^{p_o}\dot{m}_{i_o}(t) \tag{9}$$

$$\frac{dE_{ti}(t)}{dt}=\sum_{i=0}^{p_i}\dot{E}_{i_i}(t)-\sum_{o=0}^{p_o}\dot{E}_{i_o}(t)+\Phi_{h_ci}(t)-\sum_{j=0}^{n_j}\Phi_{ij_i}(t) \tag{10}$$

Here $m_i(t)$ and $E_{t_i}(t)$ are total mass and energy of the items contained in the i^{th} compartment respectively, according to the following expressions:

$$m_i(t)=\rho_i(\vartheta_i)V_i(t) \tag{11}$$

$$E_{t_i}(t)=U_i(t)+U_{w_i}(t)+E_{k_i}(t)+E_{p_i}(t) \tag{12}$$

where $U_i(t)$, $E_{k_i}(t)$ and $E_{p_i}(t)$ are internal, kinetic and potential energy of the contained fluid, respectively, whilst $U_{w_i}(t)$ is internal energy of the major part of the web girders immersed into the i^{th} fluid. Other items are: $\rho_i(\vartheta_i)$ and $V_i(t)$ fluid density and volume, ρ_S and V_{w_i} web girders density and volume, respectively.

If a web girder is immersed in the fluid, then its temperature is close to the temperature of the fluid $\vartheta_i\approx\vartheta_{w_i}$, and its internal energy can be expressed by the following formula:

$$U_{w_i}(t)=f_{w_i}c_s\rho_s V_{w_i}\vartheta_i(t) \tag{13}$$

where c_S is specific heat capacity of the web structural material.

With regard to the consideration of the thermal interaction between various ship compartments, the kinetic and potential

energy can be ignored (except in cases of fast filling or emptying of the tank), so for the total energy of the i^{th} compartment the following expression is valid:

$$E_{t_i}(t) = U_i(t) + U_{w_i}(t) \tag{14}$$

The total energy influx $\dot{E}_{i_i}(t)$ through the i_i^{th} inlet and energy efflux $\dot{E}_{i_o}(t)$ through the i_o^{th} outlet are defined by the following expressions:

$$\dot{E}_{i_i}(t) = \dot{m}_{i_i}(t)\left[h_{i_i}(t) + e_{ki_i}(t) + e_{pi_i}(t)\right] \tag{15}$$

$$\dot{E}_{i_o}(t) = \dot{m}_{i_o}(t)\left[h_{i_o}(t) + e_{ki_o}(t) + e_{pi_o}(t)\right] \tag{16}$$

In most cases, specific potential energy $e_{pi}(t) = z_i(t)g$ can be ignored, however, it is necessary to take into account specific kinetic energy, particularly during the loading and unloading, and it is defined by the formula

$$e_{ki}(t) = \alpha_{c_i}(t)\bar{v}_i^2(t)/2 \tag{17}$$

where $\alpha_{c_i}(t)$ is the kinetic energy correction factor, $\bar{v}_i(t)$ is the average fluid velocity in the cross-section pipe, and $z_i(t)$ is the height measured from the reference level.

The specific enthalpies $h_{i_i}(t)$ and $h_{i_o}(t)$ are defined by the adequate expressions depending on the existing aggregate state of the media, and generally it is valid:

$$h = u + p/\rho \tag{18}$$

It is important to note that in some cases mass inflow and outflow of the fluid for the i^{th} compartment are not prescribed, but they must be determined. Thus, during filling or emptying of the ballast tanks, the volume of air contained in the tank is changed, and consequently other thermal properties of state are changed, resulting in inflow or outflow of air. In addition, streaming of air through the related vent system occurs during unchanging volume of air and ballast, due to the existence of mechanical and thermal disequilibrium with the atmospheric air.

In general, for the determination of the air flow through the vent system it is first necessary to consider the operational sequences occurring within the existing surroundings, and then to approach the modelling of the non-isothermal streaming of air.

Due to this, to achieve a more accurate simulation of the thermal interactions occurring on the side of air into tank and vent system, it is reasonable to estimate the quasi-state nonisothermal streaming of the incompressible viscous fluid, for the mathematical modelling of which, besides the equation of state, it is also necessary to use quasi-state macroscopic balances of the mass, momentum and energy. Concerning the problem area discussed in this paper, the air streaming through the vent system can be ignored, so the air capacitance can be defined by the formula

$$C_j(t) = \frac{c_{v_a} p_a V_j(t)}{R_a T_j(t)} \tag{19}$$

By neglecting the radiation effects on the internal and external surface of the one-layer wall, only the inside and outside COTR increased for the corresponding CTR are taken into account. As the thermal capacitance of the temperature boundary layer of the fluid is negligible because it is very thin, only the thermal capacitance of the wall should be taken into account.

In some cases, like LNG tank containment system where very thick insulation layers of the primary and secondary barriers exist, and there is also a very thin layer of the invar membranes, it is necessary to use a multilayer wall for the realistic modelling of heat transfer, because the temperature gradient through insulation layers is noticeable. Thus, in the simplest case of modelling thermal interactions between LNG in the tank indexed by i and media in the j^{th} compartment, the corresponding DTNB contain besides their thermal capacitances C_i and C_j, also the following thermal capacitance: C_{ij_1} primary membrane, C_{ij_2} primary and C_{ij_3} secondary insulation layer and C_{ij_4} inner skin plating.

In this case, unsteady heat transfer through a four-layer wall between i and j is defined by the four nonlinear differential equations as follows:

$$C_{ij_l}\frac{dT_{ij_l}(t)}{dt} + \frac{T_{ij_l}(t) - T_{ij_{l-1}}(t)}{R_{ij_l}(T_{ij_{l-1}}, T_{ij_l})} + \frac{T_{ij_l}(t) - T_{ij_{l+1}}(t)}{R_{ij_{l+1}}(T_{ij_l}, T_{ij_{l+1}})} = 0, \quad l = 1,2,3,4 \tag{20}$$

where $T_{ij_l}(t)$ is unknown unsteady temperature of the l^{th} layer, whilst $R_{ij_l}(T_{ij_{l-1}}, T_{ij_l})$ is temperature dependent heat resistance between layers l and $l\text{-}1$, according to the expression:

$$R_{ij_l}(T_{ij_{l-1}}, T_{ij_l}) = \frac{\delta_{ij_{l-1}}}{2A_{ij_{l-1}}\lambda_{ij_{l-1}}(T_{ij_{l-1}})} + \frac{\delta_{ij_l}}{2A_{ij_l}\lambda_{ij_l}(T_{ij_l})} \tag{21}$$

For the first and the last layer, where COTR on the internal and external contact surfaces are taken into account, expressions (3) and (4) are valid respectively, and here given items relating to the l^{th} layer are A_{ij_l} area, δ_{ij_l} thickness and $\lambda_{ij_l}(T_{ij_l})$ temperature dependent heat conductivity, which for thinner layers can be taken as constant.

3.3 Modelling of thermal interactions when aggregate state is changed

It is necessary to indicate the change of the aggregate state that can occur during characteristic ship's operative intervals and to develop adequate mathematical models for defining unsteady thermal properties of the generated two-phase media. With respect to the upcoming thermal interactions, and the multi-component mixtures, like LNG and sea ballast, at least two-component mixtures should be accepted in order to model the acting physical processes in an authentic way.

Besides that, it is necessary to establish the corresponding mathematical models for time changeable geometric sizes, i.e. unsteady thermal interfaces, by which the influence of the unsteady intensive properties of the two-component media on its extensive properties are taken into account. In the context of the issues discussed, which are focused on the ship's operability in the low temperature surroundings and on the approach of solving the thermal problems by the application of the DTN concept, the development of the adequate mathematical model for modelling the overall thermal interactions during BF is most demanding.

For consideration of the heat exchange between two spaces having different unsteady temperatures $T_i(t)$ and $T_j(t)$, and which are mainly partitioned by a one-layer fixed wall, and sometimes, when AF, IC and BF occur, by the attachment layers, the adequate DTN can be defined. These attachment layers of the frost air,

frozen ballast and IA, characterized by unsteady thicknesses that can vary from zero to a maximum value, present added unsteady thermal resistances.

In general, if BF has to be prevented, then the ballast temperature on the contact surface having the lowest temperature must not drop below the solidification temperature at the given salinity [21], [22]. In that sense and for simplification reasons, ballast that is in its nature a multi-component mixture consisting of various salts dissolved in pure water, can be accepted (without violation of the acting physics process) as a two-component mixture of sodium chloride and water (NaCl-H_2O), for which it is inherent that during of the process of freezing pure ice is excreted from it, and consequently the salt concentration ξ_S in the remained liquid phase is increased, as illustrated in Figure 10, (based on [23]).

The process of excretion of the crystals of pure ice is started on the contact sub-cooled plate when its temperature $\vartheta_{k_{1j}}(t)$ drops below the ballast solidification temperature $\vartheta_s(t)$.

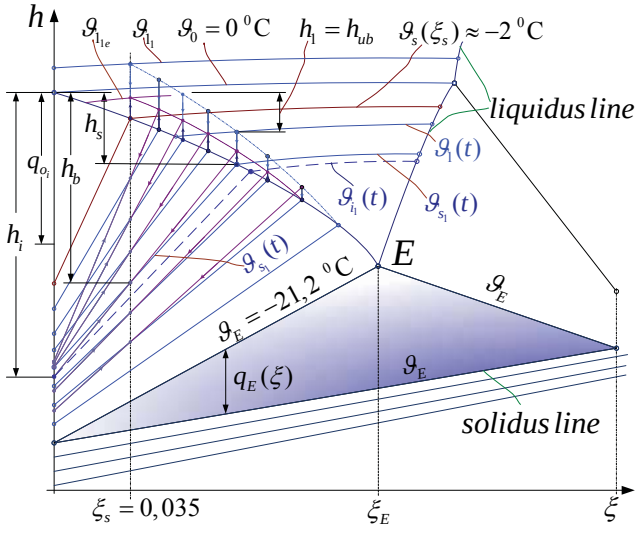

Figure 10 **Qualitative h — ξ diagram of NaCl-H_2O**
Slika 10 **Kvalitativni h — ξ dijagram za NaCl-H_2O**

When the freezing process is in progress, unsteady thickness of the excreted pure ice $\delta_{ik}(t)$ is increased and a temperature field is formed, so that the plate is being sub-cooled to the unsteady temperature $\vartheta_i(t)$ that actually presents its mean temperature, as shown in Figure 11a.

During the excretion of pure ice from the saturated ballast, the salt concentration in the remaining ballast is increased as shown in Figure 10, and practically for each new acting temperature $\vartheta_{k_{1j}}(t) < \vartheta_s(\xi_s)$ a higher concentration of salt on the liquids line is pertained.

By neglecting the influence of the temperature boundary layer on the amount of the liquid phase enthalpy of enriched brine, the enthalpy of the entire ballast is defined as follows

$$H_b(t) = m_i(t)h_i(t) + m_s(t)h_{ub}(t) \tag{22}$$

where $h_i(t)$ and $h_{ub}(t)$ are unsteady specific enthalpies of the excreted pure ice and enriched brine respectively.

The unsteady specific enthalpy of the pure ice is defined by the expression

$$h_i(t) = q_{o_i} + c_i(\vartheta_i)\vartheta_i(t) \tag{23}$$

where q_{o_i} is specific melting heat and $c_i(\vartheta_i)$ is temperature dependent specific heat capacity.

The specific enthalpy of the brine through unsaturated band depends both on the unsteady salt concentration and the unsteady temperature, so it can be defined by an approximate mathematical expression obtained on the basis the realistic $h - \xi$ diagram of mixture NaCl-H_2O as follows:

$$h_{ub}(t) = h_1\left[\xi_1(t), \vartheta_1(t)\right] = \sum_{i=0}^{8} a_i \xi_1^{i_\xi}(t)\vartheta_1^{i_\vartheta}(t) \tag{24}$$

For the determination of the masses of the extracted pure ice $m_i(t)$ and reached brine $m_S(t)$, the overall mass balance and mass balance of the salt must be used, respectively,

$$m = m_i(t) + m_s(t) \tag{25}$$

$$\xi_1 m = \xi_i\, m_i(t) + \xi_s(\vartheta_s)m_s(t) \tag{26}$$

where the salt concentration contains as follows: ξ_i of unsaturated ballast, $\xi_S = (\vartheta_s)$ of saturated ballast, and $\xi_1 = 0$ in the extracted pure ice on the sub-cooled plate.

The unsteady salt concentration in the saturated ballast depends on the saturation temperature and can be approximated by the adequate expression:

$$\xi_s(t) = \xi_s\left[\vartheta_s(t)\right] = \sum_{i=0}^{2} b_i \vartheta_s^i(t) \tag{27}$$

Figure 11 a. **The PM of the k[th] frozen plate,** b. **the corresponding DTNB**
Slika 11 a. **PM k-te zaleđene stijenke,** b. **odgovarajuća DTNB**

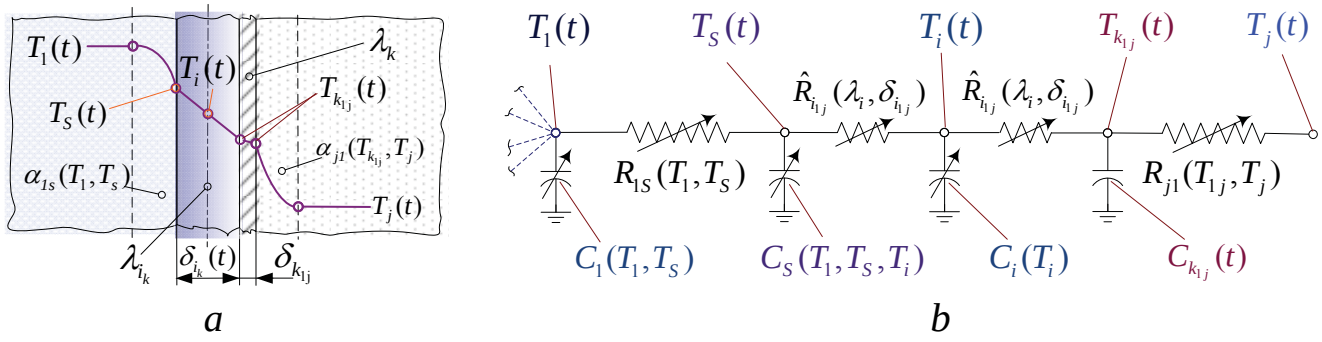

Finally, based on the above mentioned and taking into account that specific internal energy for liquids and solids is $u \approx h$ (because at relatively small pressures the term p/ρ is negligible), the unsteady internal energy of ballast is $U_b(t) \cong H_b(t)$. Since $\vartheta_{1,s,i}(t) = T_{1,s,i}(t) - T_0$, $T_0 = 273{,}15\,\mathrm{K}$, from the unsteady-state macroscopic balance of the mass it results

$$\frac{\partial m_i(T_S)}{\partial T_S} = -\frac{\partial m_s(T_S)}{\partial T_S} \tag{28}$$

and for the total time derivation of the internal energy it is obtained

$$\frac{dU_b(t)}{dt} = C_1(t)\frac{dT_1(t)}{dt} + C_S(t)\frac{dT_S(t)}{dt} + C_i(t)\frac{dT_i(t)}{dt} \tag{29}$$

In this formula the unsteady apparent thermal capacitances of unsaturated and saturated ballast, and of the excreted pure ice as well, are defined as follows

$$C_1(t) = m_s(T_S)\frac{\partial h_{ub}(T_1,T_S)}{\partial T_1} \tag{30}$$

$$C_S(t) = m_s(T_S)\frac{\partial h_{ub}(T_1,T_S)}{\partial T_S} + \left[h_i(T_i) - h_{ub}(T_1,T_S)\right]\frac{\partial m_i(T_S)}{\partial T_S} \tag{31}$$

$$C_i(t) = m_i(T_S)\frac{\partial h_i(T_i)}{\partial T_i} \tag{32}$$

By connecting these temperature dependent capacitances to the corresponding unsteady temperatures $T_1(t)$, $T_S(t)$ and $T_i(t)$ respectively, as well as taking into account the existence of the permanent thermal capacitance $C_{k_{1j}}(T_{k_{1j}})$ lumped to unsteady temperature $T_{k_{1j}}(t)$ of the partitive wall ***k***, it is possible to sketch equivalent DTNB for heat exchange between the ballast subjected to partial freezing and low temperature surroundings through the wall ***k***, as shown in Figure 11b.

The thermal resistance $\hat{R}_{i_{1j}}(\lambda_i, \delta_{i_{1j}})$ through formed pure ice of the unsteady thickness $\delta_{i_{1j}}(t)$, is defined by the expression

$$\hat{R}_{i_{1j}}(\lambda_i, \delta_{i_{1j}}) = \frac{\delta_{i_{1j}}(t)}{\bar{\lambda}_i(T_i)A_k} \tag{33}$$

where $\bar{\lambda}_i(T_i)$ is the thermal conductivity of pure ice at its mean temperature.

3.4 Modelling of environmental items interacting with the ship

A general approach to the modelling of particular environmental items, which act as excitation on the ship as a very complex energy system, is presented here.

These environmental items can be classified as non-stationary scalar and vector fields, which are a consequence of the overall energy interactions in the Solar System, and for their mathematical modelling much effort should be invested. In general, the statistical data for the characteristic environmental items in some region defined by the geographical attitude φ and longitude μ for one-year period are available from WMO (World Meteorological Organization), like those for average DAT as illustrated in Figure 2*a*.

By processing such collected data, it is possible to make adequate mathematical formulations, which pretty well approximate the spatial and time dependent environmental items. On the other hand, for a specified mission of the ship the route is predefined and can be mathematically formulated as $\varphi_r(\mu_r)$ or $\mu_r(\varphi_r)$ whichever is more appropriate, so that any environmental item can be mathematically expressed in the functional dependence on the Solar time ($\hat{t}$), and $\varphi_r(\mu_r)$ or $\mu_r(\varphi_r)$, whichever is more suitable. For instance, if the navigation route is defined by $\mu_r(\varphi_r)$, then the environmental vector and scalar quantities that are involved in mathematical models of the energy transmission between the ship and the environment are expressed by corresponding functional dependences on ρ_r and $\hat{t}$ as shown in Figure 12.

The characteristic vectors and scalars given in Figure 12 are: ***vectors*** $\vec{v}_{sc}(\varphi_r,\hat{t})$, $\vec{v}_w(\varphi_r,\hat{t})$ sea current and wind velocity, respectively (these vectors are aligned in the tangential plane of the sphere), $\vec{q}_{si}(\varphi_r,\hat{t})$ vector of the Solar irradiance; ***scalars*** $\vartheta_{a_y}(\varphi_r,\hat{t})$, $\Delta\vartheta_{a_m}(\varphi_r,\hat{t})$ and $\Delta\vartheta_{a_m}(\varphi_r,\hat{t})$ are yearly average DAT, yearly average temperature differences between max. and min. DAT, yearly average temperature differences between average max. and min. DAT, respectively, $\tau_{\Delta e}(\varphi_r,\hat{t})$ fluctuation period of the $\Delta\vartheta_{a_m}(\varphi_r,\hat{t})$, $\chi_s(\mu_r,\hat{t})$ saturation level of the moist air, $\Gamma_c(\varphi_r,\hat{t})$, $\Psi_c(\varphi_r,\hat{t})$ sky coverage with the clouds and the attenuation of the Sun radiation due to clouds, respectively, $\Gamma_{si}(\varphi_r,\hat{t})$, $\Psi_{si}(\varphi_r,\hat{t})$ sea coverage with the sea ice and sea ice thickness, respectively, $\vartheta_{s_d}(\varphi_r,\hat{t})$ sea temperature at depth d measured from free surface, $H_s(\varphi_r,\hat{t})$ i $T_s(\varphi_r,\hat{t})$ significant wave height and period, respectively.

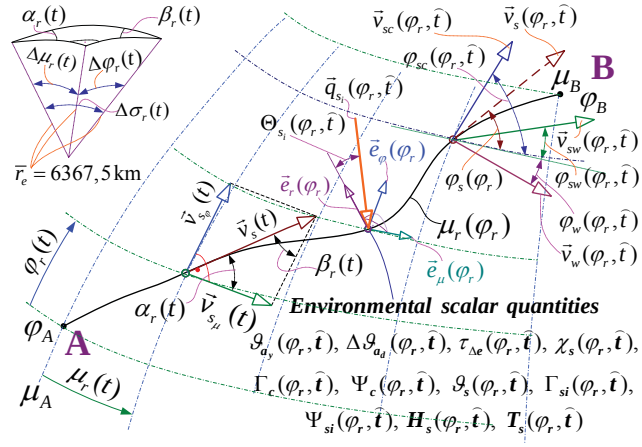

Figure 12 **The navigation route**
Slika 12 **Plovidbena ruta**

Furthermore, any vector can be defined by using the corresponding scalar, so for wind and sea currents their modules $v_w(\varphi_r,\hat{t})$ and $v_{sc}(\varphi_r,\hat{t})$, and the angles closing with related parallel $\varphi_w(\varphi_r,\hat{t})$ and $\varphi_{sc}(\varphi_r,\hat{t})$ are available, whilst for sea waves the angle between the wave propagation and related parallel $\varphi_{sw}(\varphi_r,\hat{t})$ is on disposal.

The ship's sailing velocity is a vector too, defined by the following expression,

$$\vec{v}_s(t) = \frac{d\vec{r}_s(t)}{dt} = r_e\frac{d}{dt}\left\{\begin{matrix}\cos\left[\varphi_r(t)\right]\cos\left[\mu_r(t)\right]\vec{i} + \\ +\cos\left[\varphi_r(t)\right]\sin\left[\mu_r(t)\right]\vec{j} + \sin\left[\varphi_r(t)\right]\vec{k}\end{matrix}\right\} \tag{34}$$

where $\vec{r}_s(t)$ is the radii vector of the sailing route defined by the unsteady spherical coordinates $\varphi_s(t)$ and $\mu_s(t)$ of the ship, as shown in Figure 12, and r_e is the mean radius of the Earth (here the fact that the Earth is a slightly flattened geoid is ignored). In general, taking into account that φ_r is time dependent i.e. $\varphi_r = \varphi_r(t)$, then the functional $\mu_r(\varphi_r)$ dependent on the navigation route can be expressed by either a polynomial or trigonometric series as follows:

$$\mu_r(\varphi_r) = \sum_{i_\varphi=0}^{n_\varphi} a_{i_\varphi} \varphi_r^{i_\varphi}(t), \qquad \mu_r(\varphi_r) = \sum_{i_\varphi=0}^{n_\varphi} a_{i_\varphi} \sin\left[i_\varphi \varphi_r(t)\right] \quad (35)$$

or in a special case, as in the case of orthodromic navigation, $\mu_r(\varphi_r)$ is defined by the formula:

$$\mu_r(\varphi_r) = \mu_A + \arcsin\left\{\sin(\mu_B - \mu_A)\cot(\varphi_B - \varphi_A)\tan\left[\varphi_r(t) - \varphi_A\right]\right\} \quad (36)$$

Generally, any environmental item existing on the navigation route $e_j(\varphi_r, \hat{t})$ can be expressed in dependence of $\hat{t}$ and φ_r in the form of the product of trigonometric series of the sine functions as follows:

$$e_j(\varphi_r, \hat{t}) = \sum_{i_\varphi=0}^{n_\varphi}\sum_{i_{\hat{t}}=0}^{n_{\hat{t}}}\left[A_{i_\varphi}\sin\left(i_\varphi\varphi_r + \gamma_{i_\varphi}\right)\right]\left[A_{i_{\hat{t}}}\sin\left(i_{\hat{t}}\omega_Y\hat{t} + \gamma_{i_{\hat{t}}}\right)\right] \quad (37)$$

For instance, it is possible to present the mathematical model for the atmospheric air temperature, like a combination of three basic temperature models, which are acquired from the adequate statistic data collected for some navigation route, as follows:

$$\vartheta_a(\varphi_r, \hat{t}) = \vartheta_{a_y}(\varphi_r, \hat{t}) + \frac{1}{2}\Delta\vartheta_{a_m}(\varphi_r, \hat{t})\sin\left[\omega_{sm}(\hat{t})\hat{t} + \gamma_m\right] - \frac{1}{2}\Delta\vartheta_{a_d}(\varphi_r, \hat{t})\cos\left[\omega_{sd}\hat{t} + \gamma_d(\varphi_r, \hat{t})\right] \quad (38)$$

It can be noticed in Fig. 2*b*, that the fluctuation period of $\Delta\vartheta_{a_m}(\varphi_r, \hat{t})$ is about half synodic month $\tau_{sm}(\hat{t}) = (29{,}3 \div 29{,}8)\overline{\tau}_{sd}$, where $\overline{\tau}_{sd} = 24\,h$ is mean solar day, so for the unsteady angular frequency it is obtained $\omega_{sm}(\hat{t}) = 2\pi / \tau_{sm}(\hat{t})$.

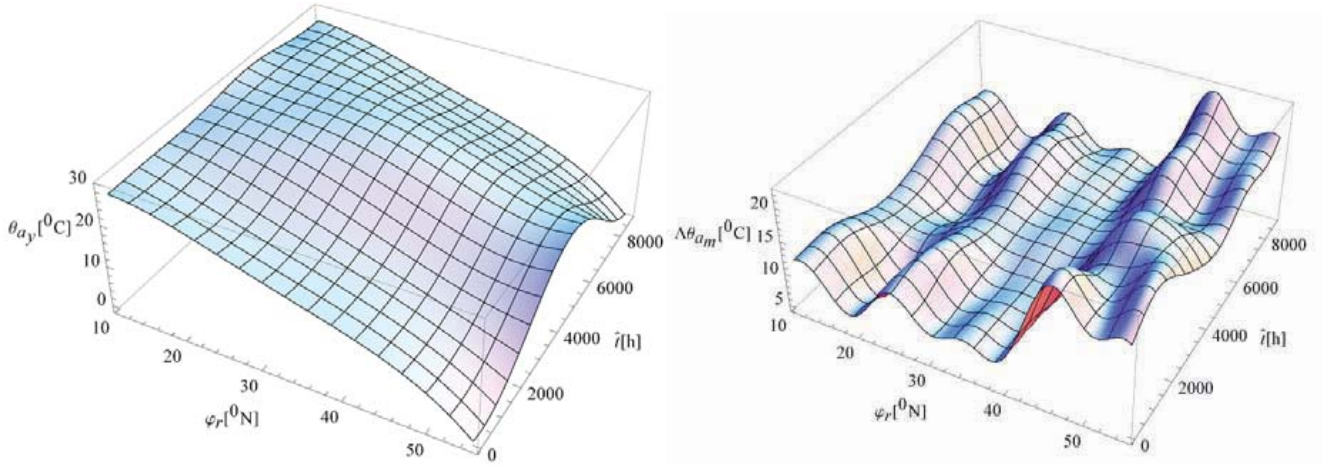

a *b*

Figure 13 **Air temperature models on the route, a. -** $\vartheta_{a_y}(\varphi_r, \hat{t})$, **b. -** $\Delta\vartheta_{a_m}(\varphi_r, \hat{t})$
Slika 13 **Temperaturni modeli zraka na ruti, a. -** $\vartheta_{a_y}(\varphi_r, \hat{t})$, **b. -** $\Delta\vartheta_{a_m}(\varphi_r, \hat{t})$

Figure 14 a. **Temp. model** $\vartheta_a(\varphi_r, \hat{t})$ **on the route,** b. **The air temperatures during the voyage**
Slika 14 a. **Temperaturni model** $\vartheta_a(\varphi_r, \hat{t})$ **na ruti,** b. **Temperatura zraka tijekom plovidbe**

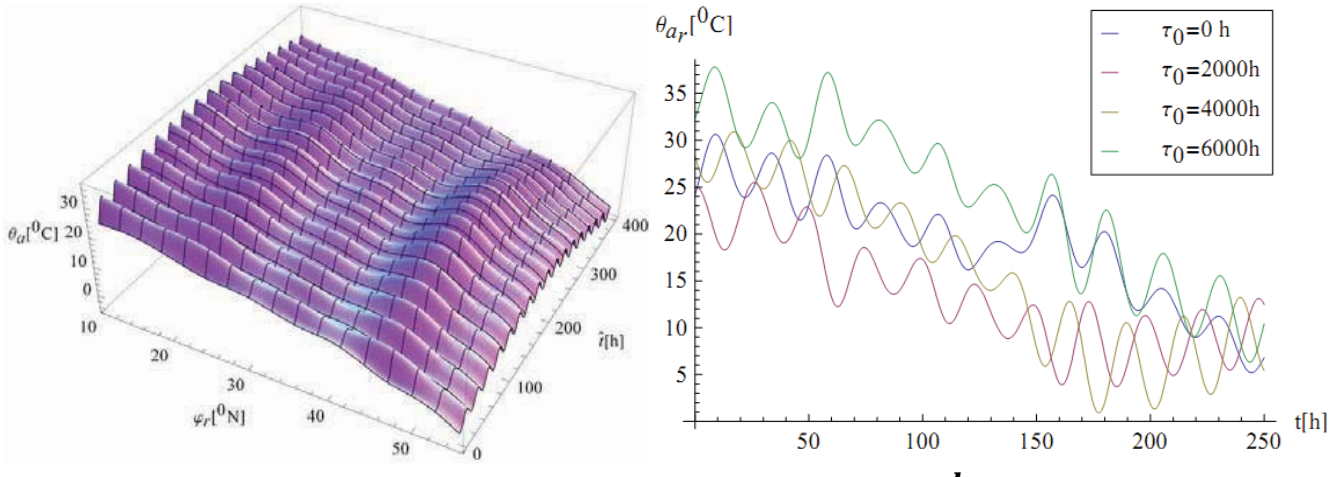

a *b*

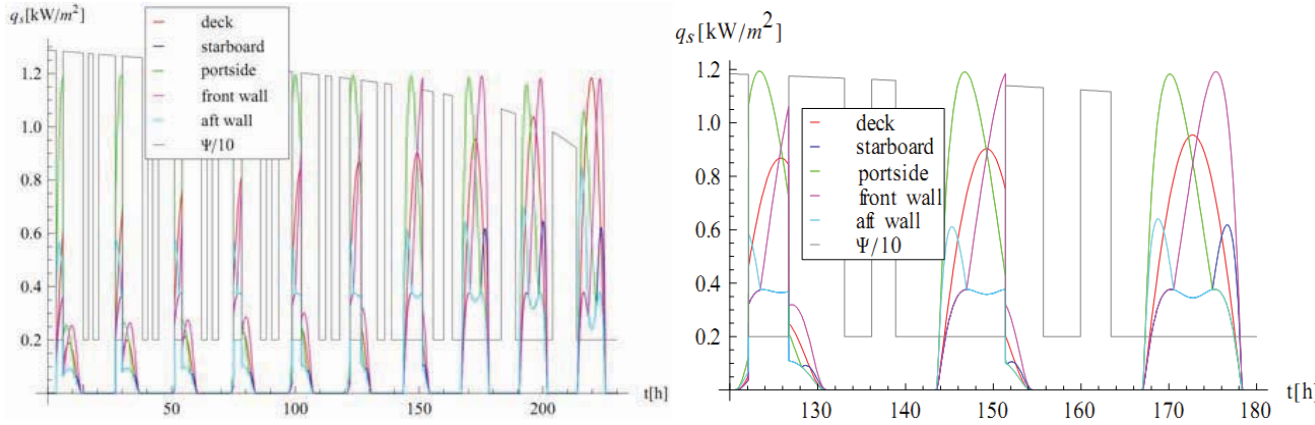

Figure 15 **Sun insolation during navigation when the sky is partly covered with clouds**
Slika 15 **Solarna insolacija tijekom plovidbe u uvjetima djelomične naoblake**

The fluctuation of $\Delta\vartheta_{a_d}(\varphi_r,\hat{t})$, can be depicted by using the fact that daily temperature minima occur right after the dawn, and their corresponding time dependent phase shift is $\gamma_d(\varphi_r,\hat{t})$, whilst the apparent angular frequency yields $\omega_{sd} = 2\pi/\bar{\tau}_{sd}$.

By using the above mentioned concept, the corresponding mathematical models for $\vartheta_{a_y}(\varphi_r,\hat{t})$ and $\Delta\vartheta_{a_m}(\varphi_r,\hat{t})$ were developed in [25] as illustrated in Figure 13 and Figure 14a.

If $t = \hat{t} - \tau_0$ is relative time, where τ_0 is time elapsed since the beginning of the year, and if $\varphi_r(t)$ is determined, then environmental items $e_j(\varphi_r,\hat{t})$ existing through the navigation route, can be expressed in the functional dependence on relative time $e_j(t)$. For instance, for the navigation starting at the moment τ_0, by inserting $\varphi_r(t)$ in the atmospheric air temperature model $\vartheta_a(\varphi_r,\hat{t})$ the time dependence $\vartheta_a(t)$ during navigation is obtained, as shown in Figure 14b. [24].

During the navigation the ship surfaces are periodically exposed to Sun's radiation that contains the following components: $q_d(t)$ intensity of the direct Sun radiation (Sun irradiance), $q_{dif}(t)$ diffuse radiation of the sky, $q_{difr}(t)$ irradiance reflected by the sea surface, and $q_{dr}(t)$ diffusely radiation of the sky. The modelling of the intensity of the total Sun radiation on the exposed ship surfaces is quite complex, especially during the navigation when the solar geometry parameters depend both on the solar time and changeable geographical position, so this is beyond the scope of this article.

This problem has been solved in a reliable manner in [24], and thus for the total Sun radiation on the characteristic ship surfaces during the navigation on a predefined route, the intermittent character is obtained as shown in Figure 15.

4 Case study – Modelling of thermal interactions between the DSBT and the surroundings

Based on Figure 4 which shows the cross section of a tanker, and by neglecting both the radiation effects and conductivity resistance through partitive walls, and taking into account the capacitances of involved thermal items, the corresponding DTN for the DSBT is obtained, as illustrated in Figure 16.

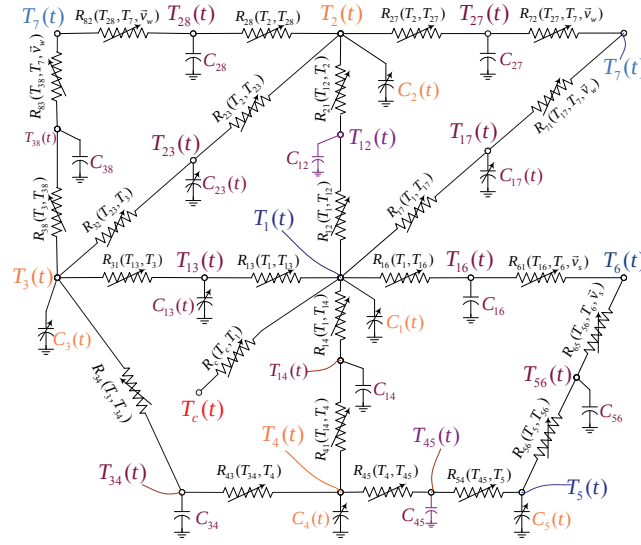

Figure 16 **DTN of the DSBT without radiation effects**
Slika 16 **DTN za DSBT bez radijacijskih utjecaja**

Thus, the underdetermined system of 17 nonlinear first order differential equations with 18 unknown temperature functions is obtained. It should be noted that the above mentioned artificial walls numbered with ***12*** and ***45*** have been introduced into the system of differential equations in order to avoid the combined system of nonlinear ordinary and differential equations, which is more complex for solving than the system containing only differential equations. Further, two characteristic cases of the application of this system of differential equations will be considered, the first case when there is no heating of the ballast tanks, and second, when there is heating of the ballast tanks.

4.1 No heating of the ballast tanks

No ballast freezing

In this case, navigation without the ballast tank heating is considered, so in the mathematical view $T_c(t) = T_1(t)$, the

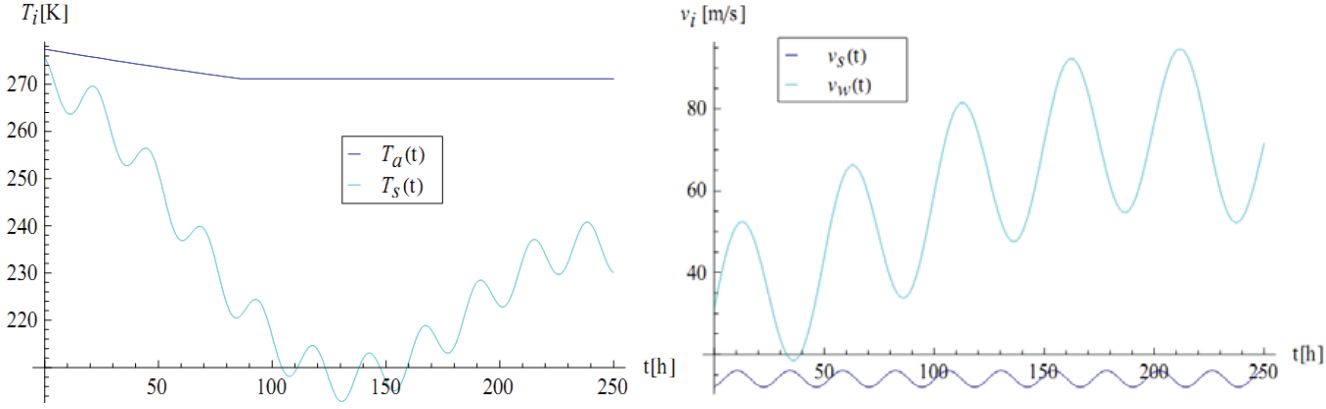

Figure 17 **The unsteady air and sea temperatures as well as wind and sea currents velocities**
Slika 17 **Neustaljene temperature zraka i mora te brzine vjetra i morskih struja**

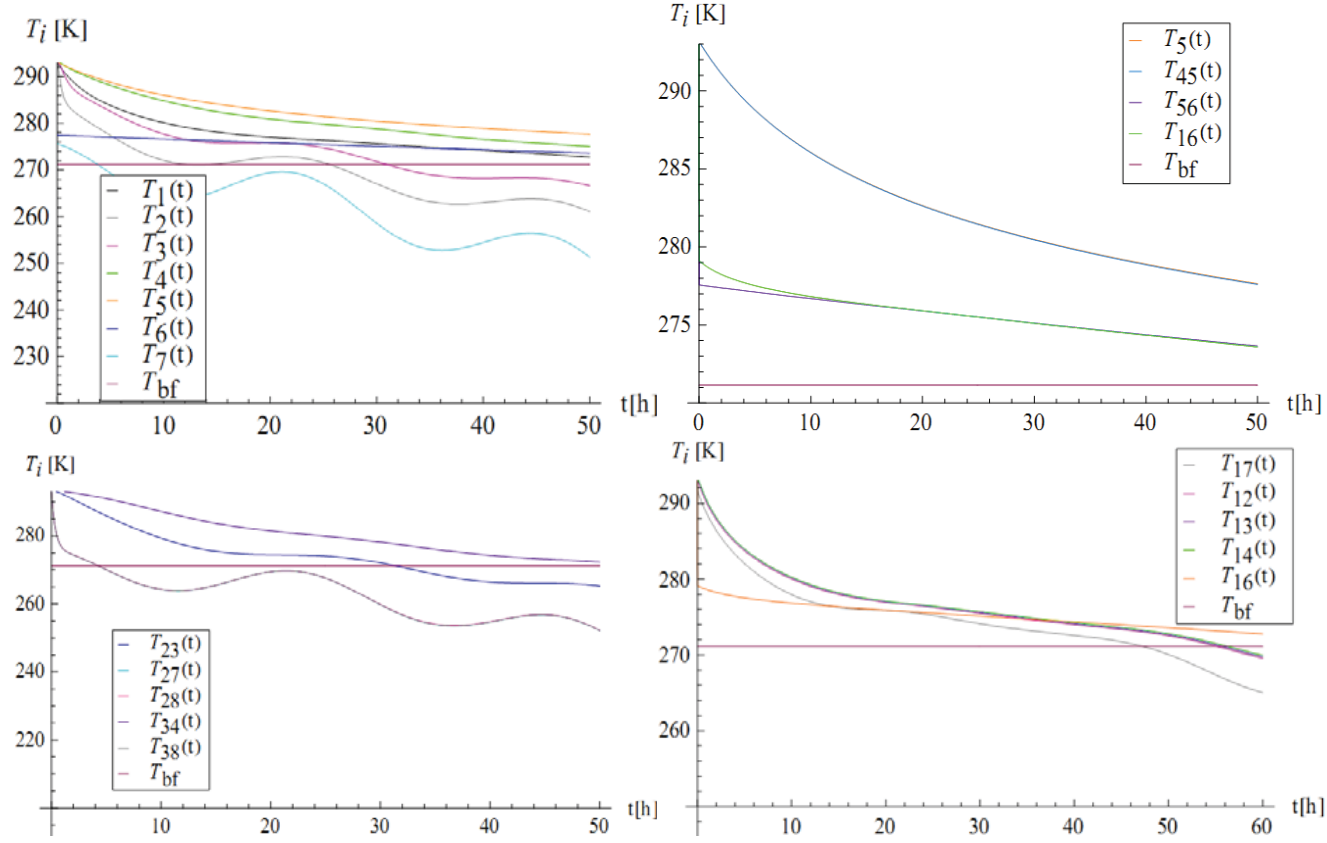

Figure 18 **Unsteady temperatures of typical items in the unheated ballast tanks**
Slika 18 **Neustaljene temperature karakterističnih stavki negrijanih balastnih tankova**

underdetermined system of the differential equations becomes a determined system. The characteristic environment items that are in thermal interacting with the ballast tanks are defined in the way as shown in Figure 17.

Based on arbitrarily chosen same initial conditions for all unknown unsteady temperatures, and by using the software package *Mathematica7* their solutions are obtained, as illustrated in the diagrams in Figure 18. According to these temperature diagrams, it is evident that the underlying ballast solidification temperatures firstly appeared on wall ***17***, so by finding the root transcendental equation $T_{17}(t) = T_{bf}$, the time interval at which freeze does not occur is obtained.

Ballast freezing on plate 17 (the I-phase of freezing)

The adequate DTN describing the heat transfer between the ballast in the freezing process and the surroundings is drawn, as shown in Figure 19. Based on this DTN, taking that $T_1(t) = T_C(t)$

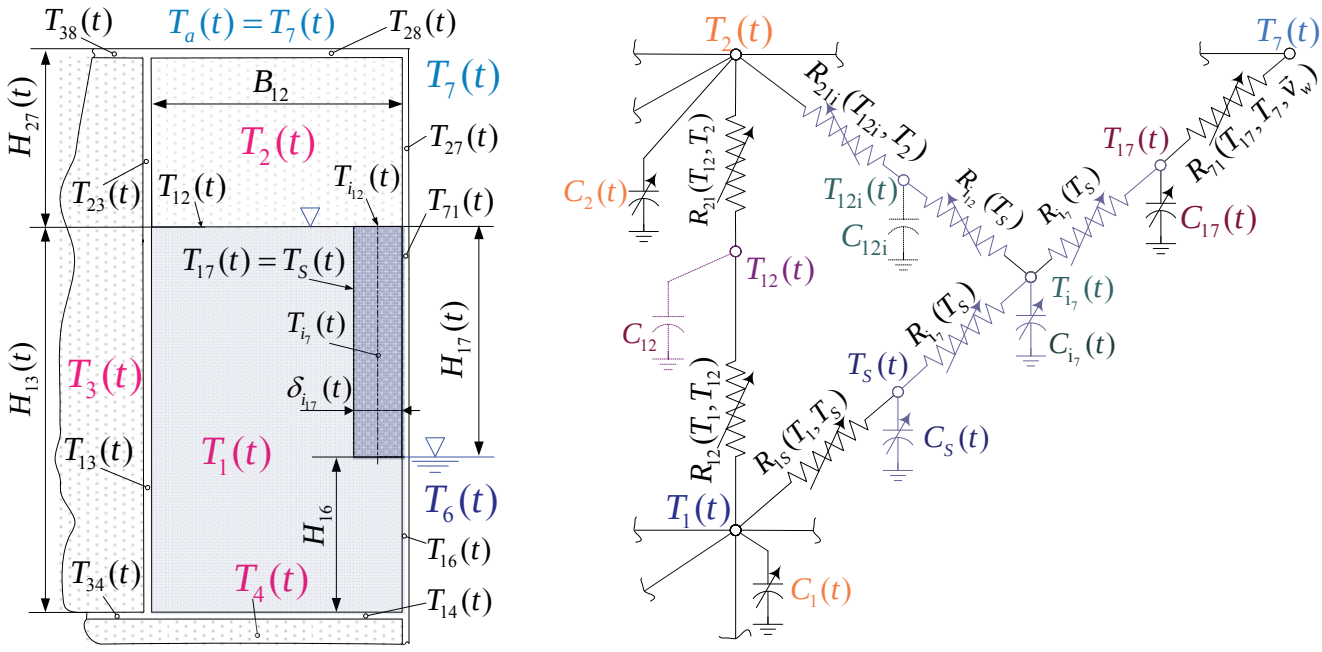

Figure 19 **The PM and corresponding DTN for the DSBT during BF on plate 17**
Slika 19 **PM i odgovarajuća DTN za DSBT tijekom BF na stijenci 17**

Figure 20 **Unsteady temperatures during the first phase of freezing**
Slika 20 **Neustaljene temperature tijekom prve faze zaleđivanja**

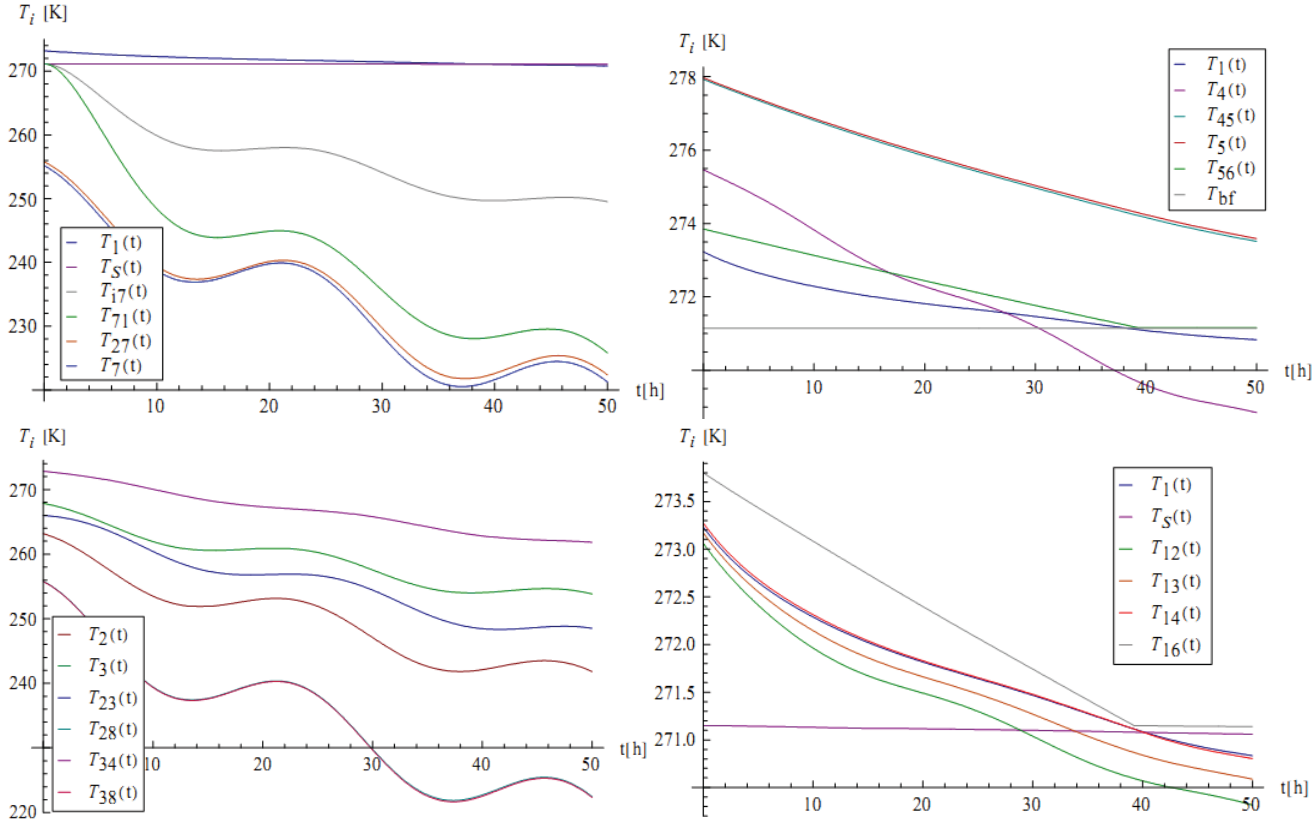

and neglecting the heat transfer through node ***12i*** (because there is a very thin layer of the extracted ice), the determined system of 20 nonlinear differential equations that is solvable only numerically is obtained.

Initial conditions for unknown unsteady temperatures T1(t), $T_2(t)$,…$T_{56}(t)$, correspond to the values at the end of the previous interval (then there is no BF), which been computed for the time corresponding to the root equation $T_{17}(t) = T_{bf}$, $\Rightarrow t_I = 47,2h$. These time depending temperatures during the first phase of freezing are shown in Figure 20, from which it is evident that further freezing will occur on artificial wall ***12***. During this phase of freezing the solidification temperature of the ballast $T_S(t) = T_{bf}$ is slowly reduced, because the salt concentration $\xi_s(t)$ in the unfrozen ballast is slightly increased, as shown in Figure 21b.

The time interval of this freezing phase is easily achieved by finding the transcendental equation root $T_{12}(t) = T_S(t)$, that is $t_{II} = 28,67\,\text{h}$, and for the thickness of the extracted ice on the wall ***17*** at the end of this freezing phase $\delta_{i7(t_{II}=28,67)} = 0,141\text{m}$ is obtained, as shown in Figure 21a.

It should be noted that in this phase of BF, instead of temperature $T_{17}(t)$ of wall ***17***, which is valid in the case without freezing, the temperature $T_{71}(t)$ is corresponding temperature for wall ***17***, so temperature $T_{17}(t)$ from the previously non-freezing phase corresponds to solidification temperature $T_S(t)$ during this freezing phase, and here $T_{i7}(t)$ is the unsteady mean temperature of the excreted pure ice on the internal surface of wall ***17***.

4.2 The heating of the ballast tanks without BF

In this case, the dynamic thermal interactions between the heated ballast tanks and the surroundings are considered. In order to prevent BF, quasistatic balance temperature $T_1(T_7, v_w)_{(T_{17}=T_{bf})}$ shown in Figure 22, is taken as the equilibrium unsteady temperature of the ballast, and because of that the above mentioned system of differential equations is reduced. Firstly, as the time dependence $T_1(t) = T_1\left[T_7(t), v_w(t)\right]_{(T_{17}=T_{bf})}$ is predefined, the first differential equation is transformed into an ordinary transcendental equation from which the unknown unsteady temperature $T_c(t)$ is obtained. Secondly, the differential equations in node ***17*** vanished because the corresponding temperature in that node is $T_{17} = T_{bf} = const.$, and consequently the determined system of differential equations containing 15 unknown unsteady temperatures $T_2(t)$, $T_3(t)$,… $T_{56}(t)$ is obtained.

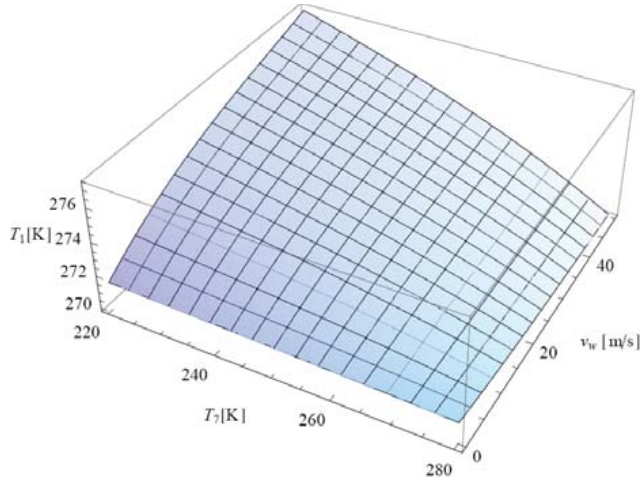

Figure 22 **The dependence of the quasistatic balance temperature on the air temperature and wind velocity**
Slika 22 **Ovisnost kvazistatičke ravnotežne temperature balasta o temperaturi zraka i brzini vjetra**

For unsteady environmental items such as ship sailing velocity (or sea current velocity), wind velocity, and temperatures of the atmospheric air and sea, as shown in Figure 17, the solution of this system of differential equations is presented in Figures 23a.,b.,c., whilst the effect of the unsteady temperatures on some CHTC is shown in Figure 23d.

Finally, based on the balanced temperature of the heating coil, the total unsteady heating load of the side ballast tank $\Phi_{tot}(t) = \sum \Phi_{1j}(t)$ can be determined, as shown in Figure 24. This heating load is consists of the heating flows through walls ***17***, ***12***, ***16***, ***13***, ***14***, and of the heating flow (ballast capacitance) that is accumulated in the ballast $\Phi_c(t)$. It can be seen from Figure 24 that the majority of the total heating load consists of the heating flows through wall ***17*** because of the highest temperature difference, and through wall ***16*** because of the lowest convective resistances.

Figure 21 a. **The ice thickness on wall 17,** b. **The salt concentration in the ballast**
Slika 21 a. **Debljina leda na stijenci 17,** b. **Koncentracija soli u balastu**

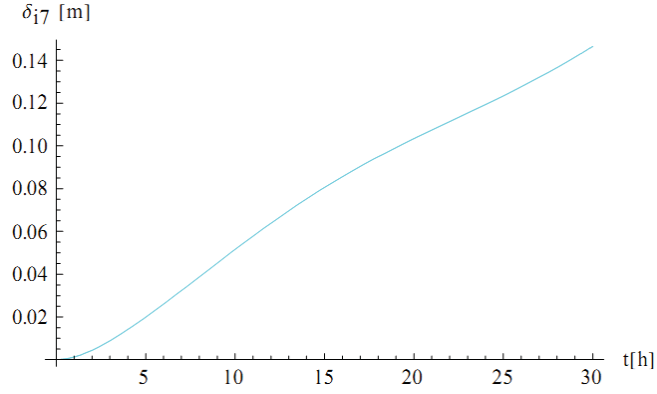

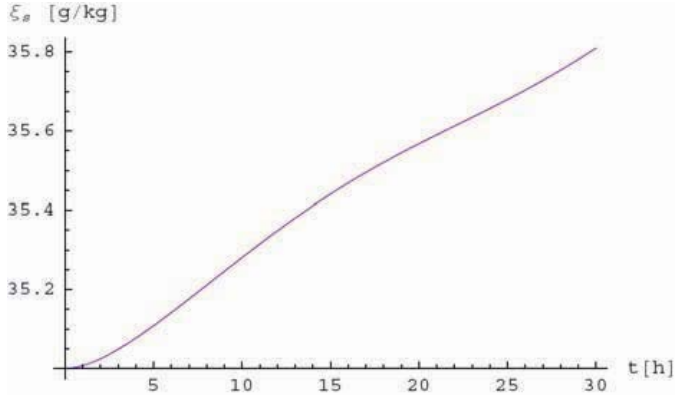

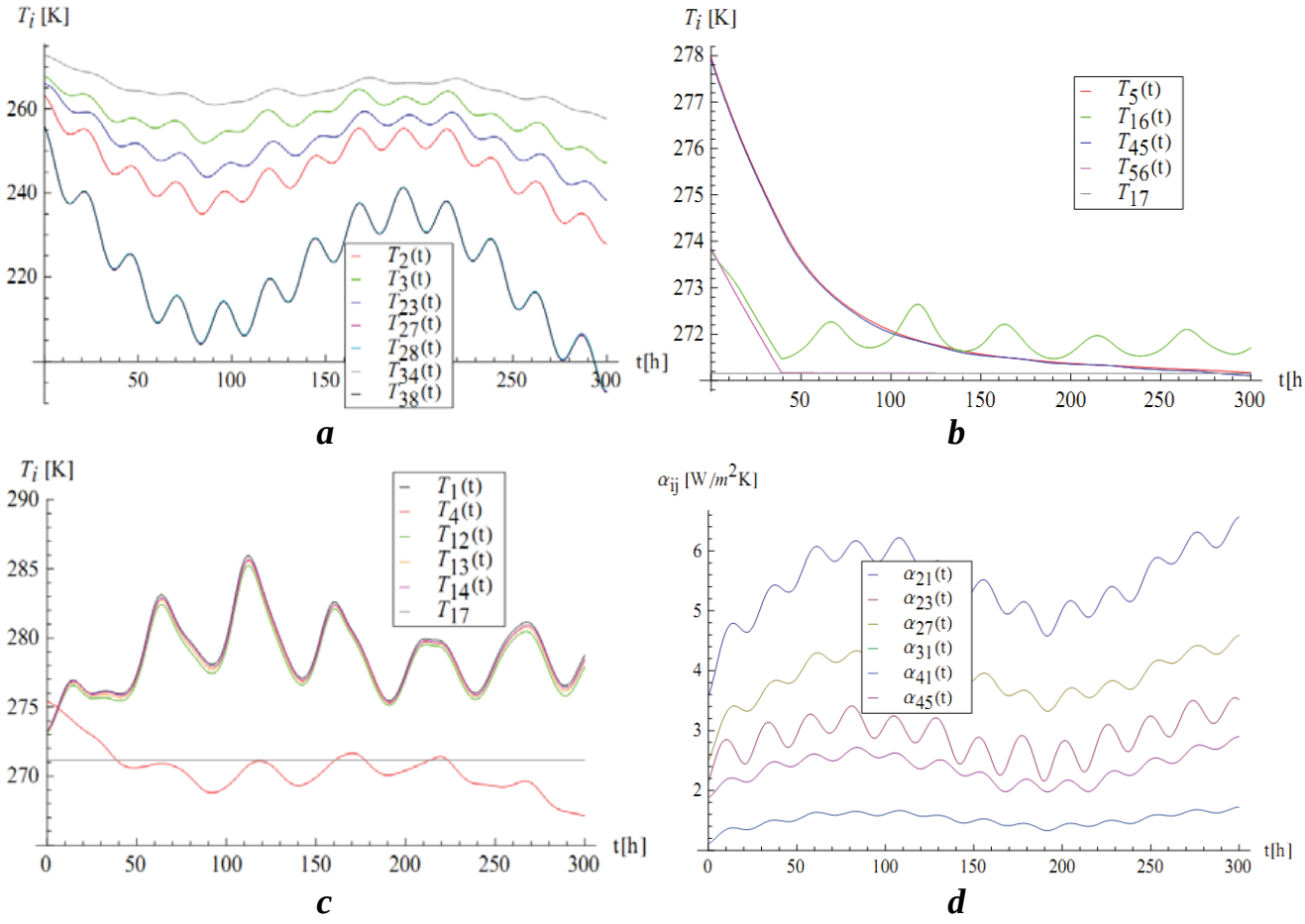

Figure 23 a., b., c. **Unsteady temperatures of typical items in heated DSBT,** d. **Typical unsteady CHTC**
Slika 23 a., b., c. **Neustaljene temperature karakterističnih stavki u grijanom DSBT, d. Karakteristični neustaljeni CHTC**

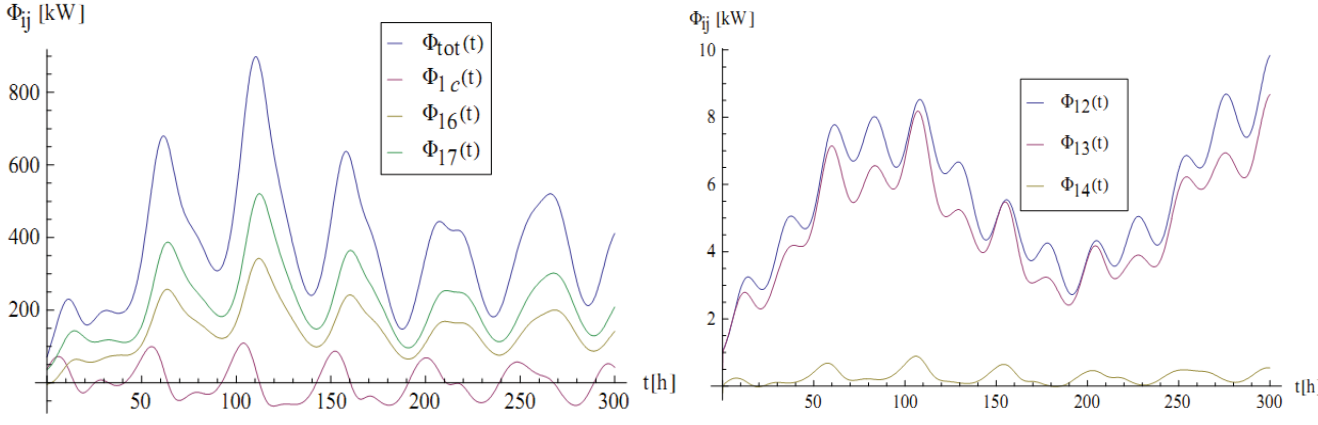

Figure 24 **The unsteady, total heat load and individual heat loads of the ballast tank**
Slika 24 **Neustaljeno ukupno i pojedinačna toplinska opterećenja balastnog tanka**

5 Conclusion

The article presents an approach to the modelling of thermal interaction between the ship and the low-temperature environment in order to perceive acting problems that need to be overcome already in the preliminary design phase. The most important problems are related to the parts of the hull and some equipment and facilities exposed to the extreme low-temperature effects, as well as substantial amounts of acting heat loads of specific ship systems (ballast, liquid fuel, ship's quarters, etc.).

By creating credible mathematical models of thermal interactions of the ship in a realistic environment, it is possible to obtain

close to realistic thermal responses of the ship, on the basis of which the selection of appropriate structural materials can be assessed, and the ship's thermal plant capacity necessary to balance the overall acting heating load can be determined.

The concept of application of DTN in the modelling of the thermal interactions allows the elaboration of extremely complex thermal problems in a rather simple and tangible way, so that the thermal system is described with a system of highly nonlinear differential equations the solutions of which are time-dependent temperatures.

These solutions are achieved only by appropriate numerical methods, and for this purpose the software package *Mathematica7*, which in a relatively short period of time gives very accurate results, has been used.

The most realistic insight into the upcoming thermal interaction is achieved by applying the concept of DTN extended to radiation effects, which is not considered in this article. The most interesting and probably the most complex and most useful is the application of this concept in the modelling of thermal interaction between LNG carriers and the environment, which is reflected through the simulation both of the temperature field in the hull and the unsteady heating loads of the cargo tanks, in order to facilitate the selection of the solution for the cargo containment system, and thus further research in this direction is expected.

Acknowledgment

The author sincerely thanks the Research Department of *Bureau Veritas*, for the semi-annual hospitality, which enabled him to devote himself to scientific research related to the issues being considered in this article.

References

[1] GOSPIĆ, I.: ″Modeling of Tanks Heating Loads on the Vessels Operating in Arctic Region", NT, ATA 1223A, Technical Note, Marine Division Bureau Veritas, Paris, 2009.
[2] LARSEN, L.L.: ″Development with Ice Class LNG Designs″; SMM, Hamburg, September 2006.
[3] KOREN, J.V.: ″Winterization of LNG Carriers″; Tanker Operator Conference, Oslo, June, 2007.
[4] SODHI, D.S.: ″Northern Sea Route Reconnaissance Study-A Summary of Icebreaking Technology″; Special Report 95-17, Us Army Corps of Engineers, June, 1995.
[5] MULHERIN, N.D., SODHI, D.S., SMALLIDGE, E.: ″Northern Sea Route and Icebreaking Technology – An Overview of Current Conditions″; Special Report 96-4, Us Army Corps of Engineers, June, 1996.
[6] MULHERIN, N.D.: ″Northern Sea Route –Its Development, and Evolving State of Operations in the 1990s.″; Special Report 97-5, Us Army Corps of Engineers, June, 1997.
[7] MAHMOOD, M., REVENGA, A.: ″Design Aspects of Winterized and Arctic LNG Carriers–A Classification Perspective″; Proceedings of OMAE, Hamburg, 2006.
[8] SAARINEN, S., RANKI, E.: ″General Description of Ice Condition in Gulf of Bothnia, Gulf of Finland, Pechora Sea and Kara Sea″; AARC Report K-66b, Nov. 2007.
[9] JOHANSTON, M., FREDERKING, R., TIMCO, G.: ″Properties of Decaying First Year Sea Ice, Two Seasons of Field Measurements", 17th Int. Symposium on Okhotsk Sea and Sea Ice, Momebetsu, Japan, Feb., 2002.
[10] TIMCO, G.W., JOHNSTON, M.E.: ″Sea Ice Strength during the Melt Season″; Proceedings of the 16th IAHR International Symposium on Ice, Dunedin, New Zealand, December, 2002.
[11] ELO, M.: ″General Description of Ice Condition in the Beaufort Sea, Chukchi Sea and Bearing Sea″; AARC Report K-79b, 2007.
[12] EVGENY, A.: ″Scientific Aspects of LNG Arctic Carriers' Design″; 2nd Annual Conference Arctic Shipping, St. Petersburg, Russia April, 2006.
[13] DNV, Pt.5, Ch1, Sec.6: ″Winterization–Rules for Classification of Ships″; Det Norske Veritas, August, 2006.
[14] KOREN, J.V: ″Winterization of LNG Carriers″; Tanker Operator Conference, Oslo 2007.
[15] JONES, K.F., ANDREAS, E.L.: ″Sea Spray Icing of Drilling and Production Platforms″; ERDC/CRREL TR-09-03, Us Army Corps of Engineers, February, 2005.
[16] GERWICH, B.C.: ″Construction of Marine and Offshore Structures", CRC Press, New York, 2000.
[17] MILLS, A.F.: ″Basic Heat and Mass Transfer", Irwin, Chicago, London, 1992.
[18] JANNA, W.S.: ″Engineering Heat Transfer", CRC Press, London, 2000.
[19] MCGUIRE, WHITE: ″Liquefied LNG Handling Principles on Ships and in Terminals", Witerby, London, 2000.
[20] BIRD, R.B., STEWART, W.E., LIGHFOOT, E.N.: ″Transport Phenomena″; John Wiley & Sons. Inc, New York, 1960.
[21] UNESCO technical papers in marine science: ″Algorithms for Computation of Fundamental Properties of Seawater″, Unesco 1983.
[22] MIRONENKO, M.V., GRANT, S.A., MARION, G.M., FARREN, R.E.: ″FREZCHEM2 – A Chemical Thermodynamic Model for Electrolyte Solutions at Subzero Temperatures″; CRELL Report 97-5, Us Army Corps of Engineers, October, 1997.
[23] BOŠNJAKOVIĆ, F.: ″Nauka o toplini III dio", Tehnička knjiga, Zagreb 1986.
[24] GOSPIĆ, I.: ″Modeling of Marine Diesel Engine Trigeneration Energy Systems", Dissertation, Zagreb 2008.